Report

Current Biology

The geologic history of primary productivity

Highlights

- The biosphere has fixed $\sim10^{11}$–10^{12} Gt C via primary production over Earth's history
- $\sim10^{39}$–10^{40} cells have existed on Earth since the origin of life
- Cyanobacteria are likely the most abundant group of organisms to have ever existed
- Changes in productivity should be considered in the use of molecular clocks

Authors

Peter W. Crockford, Yinon M. Bar On, Luce M. Ward, Ron Milo, Itay Halevy

Correspondence

petercrockford@cunet.carleton.ca

In brief

Crockford et al. quantify the historically integrated productivity of the biosphere. In total, Earth's biosphere has fixed $\sim10^{11}$–10^{12} billion tonnes of carbon, which is $\sim$100 times Earth's entire carbon stock. Crockford et al. further estimate that there have been $\sim10^{39}$–10^{40} cells on Earth to date, with cyanobacteria being the most abundant group.

Crockford et al., 2023, Current Biology *33*, 4741–4750
November 6, 2023
https://doi.org/10.1016/j.cub.2023.09.040

CellPress

Current Biology

CellPress

Report

The geologic history of primary productivity

Peter W. Crockford,[1,2,3,6,7,*] Yinon M. Bar On,[2,4] Luce M. Ward,[5] Ron Milo,[2] and Itay Halevy[2]
[1]Department of Earth Sciences, Carleton University, Ottawa, ON K1S 5B6, Canada
[2]Department of Earth and Planetary Sciences, Weizmann Institute of Science, 7610001 Rehovot, Israel
[3]Department of Marine Chemistry and Geochemistry, Woods Hole Oceanographic Institution, Woods Hole, MA 02543, USA
[4]Division of Geological Sciences, California Institute of Technology, Pasadena, CA 91125, USA
[5]Department of Geosciences, Smith College, Northampton, MA 01063, USA
[6]X (formerly Twitter): @Earth2Pete
[7]Lead contact
*Correspondence: petercrockford@cunet.carleton.ca
https://doi.org/10.1016/j.cub.2023.09.040

SUMMARY

The rate of primary productivity is a keystone variable in driving biogeochemical cycles today and has been throughout Earth's past.[1] For example, it plays a critical role in determining nutrient stoichiometry in the oceans,[2] the amount of global biomass,[3] and the composition of Earth's atmosphere.[4] Modern estimates suggest that terrestrial and marine realms contribute near-equal amounts to global gross primary productivity (GPP).[5] However, this productivity balance has shifted significantly in both recent times[6] and through deep time.[7,8] Combining the marine and terrestrial components, modern GPP fixes ≈250 billion tonnes of carbon per year (Gt C year^{-1}).[5,9–11] A grand challenge in the study of the history of life on Earth has been to constrain the trajectory that connects present-day productivity to the origin of life. Here, we address this gap by piecing together estimates of primary productivity from the origin of life to the present day. We estimate that ~10^{11}–10^{12} Gt C has cumulatively been fixed through GPP (≈100 times greater than Earth's entire carbon stock). We further estimate that 10^{39}–10^{40} cells have occupied the Earth to date, that more autotrophs than heterotrophs have ever existed, and that cyanobacteria likely account for a larger proportion than any other group in terms of the number of cells. We discuss implications for evolutionary trajectories and highlight the early Proterozoic, which encompasses the Great Oxidation Event (GOE), as the time where most uncertainty exists regarding the quantitative census presented here.

RESULTS AND DISCUSSION

A first step to summing up the cumulative efforts of the biosphere is the identification of key events that have caused large shifts in global productivity. The first key event is when oxygenic photosynthesis came to dramatically outpace other autotrophic metabolisms and thus increase global productivity. Isotope-based proxies[12,13] and sedimentary features[14,15] provide a conservatively late estimate for oxygenation of Earth's surface and the rise of oxygenic photosynthesis to dominance ≈2.4 billion years (Ga) ago.[16,17] Another critical moment is the rise of algae to ecological prominence, ≈800–650 million years ago.[18–20] We note that there have been suggestions that both the rise to prominence of oxygenic photosynthesis and the transition to algal-dominated ecosystems occurred much earlier in Earth's past.[21–26] A third critical transition is when land plants colonized the continents,[7] dated to ≈450–350 million years ago.[27–29] In contrast to these ecological and productivity leaps are catastrophic declines, such as "snowball Earth" episodes,[30,31] and major extinctions.[32,33]

We created a "most probable trajectory" based on a synthesis of literature sources and found an overall increase in primary productivity over Earth's history (Figure 1A; see STAR Methods).[6–8,13,34–51] A possible exception to a stepped, near-monotonic productivity increase is the early Proterozoic (≈2.4–2.0 Ga ago) where estimates span over three orders of magnitude.[42] The reason for this large range is that some productivity estimates incorporate the hypothesis of an atmospheric O_2 and productivity "overshoot" across the Great Oxidation Event (GOE),[52,53] whereas others do not.[51] The long duration of this interval, combined with the wide range in productivity estimates, introduces the greatest uncertainty into our calculations. Other sources of uncertainty, such as an assumption of a fixed gross primary productivity (GPP):net primary productivity (NPP) ratio (Box 1), are far smaller than the range of individual estimates.

How much carbon has Earth's biosphere ever fixed?

Integrating the most probable productivity trajectory (Figure 1A), which does not include a high-productivity GOE, we estimate that ≈2 × 10^{11} Gt C have ever been fixed by the biosphere through GPP. Considering the full uncertainty envelope for both high- and low-productivity GOE scenarios and including scenarios of an early and productive emergence of oxygenic photosynthesis (Figure 1A), this range expands to ~10^{11}–10^{12} Gt C. To place our most probable estimate into perspective, our results reveal that an amount of carbon equivalent to Earth's entire carbon stock (≈3 × 10^9 Gt C)[59] has been taken up through

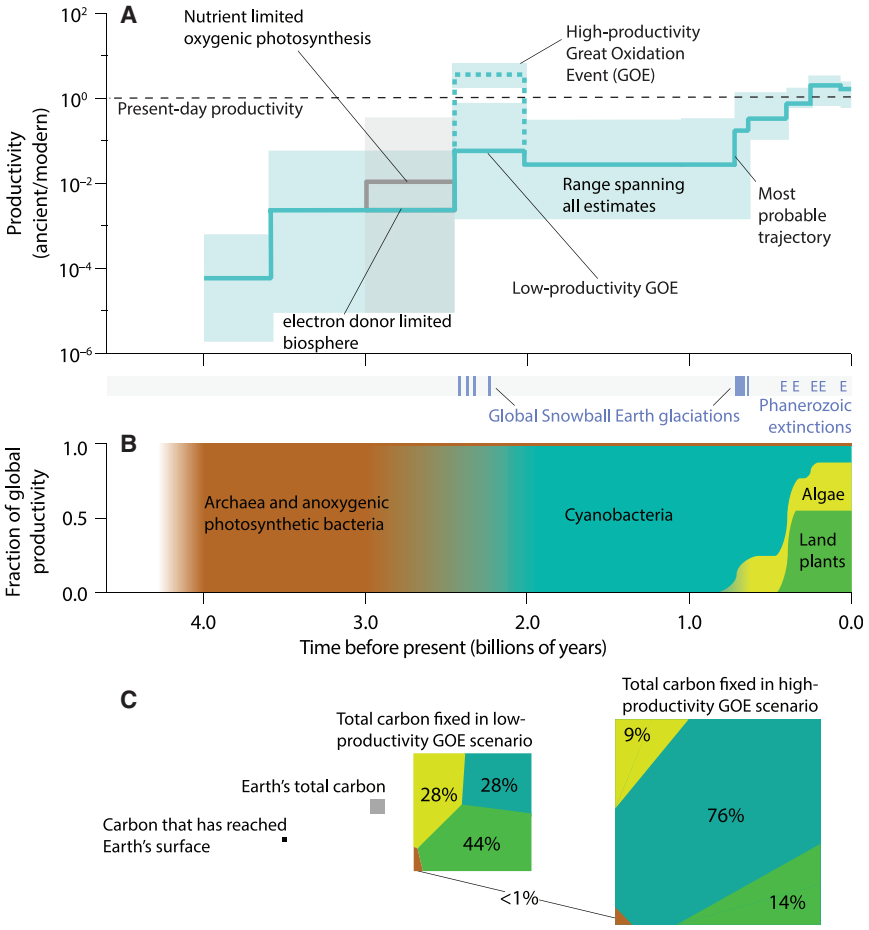

Figure 1. The geologic history of primary productivity

(A) Estimates of primary productivity against time in billions of years before the present. Net and gross paleoproductivity estimates are grouped together through the assumption of a fixed GPP:NPP ratio (Box 1) and are normalized to modern productivity. The blue line shows our estimated most probable trajectory, and the light blue envelope spans the range of literature estimates. An alternative scenario from 3 Ga ago to the GOE, which includes model estimates of productive Archean oxygenic photosynthesis, is shown in gray. Panglacial ("snowball Earth") episodes and major Phanerozoic extinction intervals are marked below (A).

(B) The fraction of global productivity of archaea and anoxygenic bacteria (including chemolithotrophs), cyanobacteria, algae, and land plants for the most probable trajectory.

(C) Historically integrated productivity contributions of the major primary producer groups for the most probable trajectory. The size of the squares corresponds to the integrated mass of carbon. Also shown in (C) are Earth's total carbon stock (small gray box) and an estimate of how much carbon has reached Earth's surface from its interior by degassing of mantle carbon (smaller black box).

See also Data S2 and S3.

primary productivity ~100 times since the origin of life. To highlight the importance of the contribution of oxygenic photosynthesis to this cycling effort, if the low level of pre-oxygenic photosynthetic productivity (Figure 1A) continued to the present day, the global biosphere would have only cycled this amount once. Moreover, stoichiometrically converting fixed carbon into an estimate of gross O_2 production suggests that Earth's biosphere has produced ~10^5–10^6 times the modern atmosphere's O_2 content, equivalent to ~10 times the integrated O_2 equivalents in the exosphere (crust, surface, and fluid envelopes) and mantle.[60] Thus, of the total O_2 ever produced, an order of magnitude more has been consumed by aerobic respiration than has accumulated in the ocean-atmosphere or that has been consumed through the oxidation of reduced volcanic and hydrothermal exhalations and ferrous iron in rocks that now reside in Earth's exosphere and mantle. Importantly, this calculation further implies that since the emergence of oxygenic photosynthesis, ~10% of all organic matter ever produced has been consumed via anaerobic respiration, which deviates from the modern environment, where only ~1% is respired anaerobically.

Interestingly, we find that accounting for periods following mass extinctions or snowball Earth episodes, which have a summed duration of ~10^8 years,[31,61] has only had a minor influence on the summed productivity of Earth's biosphere. Moreover, if major evolutionary innovations were driven by environmental calamity,[62,63] and if this allowed for new environmental niches to be colonized by life, it seems reasonable that a legacy of these "death" events has been an overall increase in the size and productivity of Earth's biosphere.[64]

The Earth's productivity has been mostly cyanobacterial

Who has been the dominant productivity contributor throughout Earth's history? Today, primary productivity is dominated by terrestrial plants, followed by marine algae, followed by cyanobacteria (Figure 1B).[5,9,65] Projecting distributions back in time is complicated by uncertainties of when different primary producers emerged to ecological prominence. Depending on the timing of algal dominance of marine productivity and land plant dominance of overall productivity, a low-productivity GOE trajectory suggests that land plants have dominated total productivity over time (Figure 1C; Table 1; see also STAR Methods). However, no matter when significant algal or land plant populations emerged, a high-productivity GOE trajectory leads to cyanobacterial dominance of integrated total productivity (Figure 1C; Table 1).

We note that the relative contribution of cyanobacterial productivity is likely underestimated for several reasons. First, modern terrestrial productivity is known to have been much lower in Earth's recent past (e.g., during Quaternary ice ages).[6] Second, if ancient oceans experienced lower nutrient levels or higher temperatures,[43] it is plausible that cyanobacteria contributed a larger proportion of global primary productivity relative to algae

Box 1. Definitions and characteristic values of modern GPP and NPP

Definitions of primary productivity as well as modern estimates of marine and terrestrial gross primary productivity (GPP) and net primary productivity (NPP) are provided below. Discussion of modern ratios of GPP to NPP is also included.

Productivity is measured and defined in different ways.[11,54] We briefly summarize productivity definitions[55] and recent estimates of their values on the modern Earth, in gigatonnes of carbon per year (Gt C $year^{-1}$ = 10^{15} g C $year^{-1}$ = Pg C $year^{-1}$). As oxygenic photosynthesis (Equation 1) dominates modern primary production, other metabolisms are neglected due to their relatively insignificant contribution.[56]

$$6CO_2 + 12H_2O \rightarrow C_6H_{12}O_6 + 6H_2O + 6O_2. \quad \text{(Equation 1)}$$

Gross primary productivity (GPP) is defined as either the rate of organic carbon production or the rate of oxygen production during water splitting in photosystem II by autotrophs in an ecosystem, after photorespiration but before autotrophic respiration.[57]

Modern global GPP ≈ 250 Gt C $year^{-1}$.

Marine ≈ 100–150 Gt C $year^{-1}$, terrestrial ≈ 100–150 Gt C $year^{-1}$.

Net primary productivity (NPP) is defined as the amount of organic matter production after autotrophic respiration (i.e., GPP minus autotrophic respiration).

Modern global NPP ≈ 120 Gt C $year^{-1}$.

Marine ≈ 60 Gt C $year^{-1}$, terrestrial ≈ 50–60 Gt C $year^{-1}$.

GPP:NPP is the ratio of GPP to NPP, which is not constant and varies as a function of location, season, and year in both terrestrial and marine biomes. Compiled estimates[11] suggest a GPP:NPP value of 2.1 (2.0 marine, 2.3 terrestrial). This value is consistent with a recent global synthesis of terrestrial GPP:NPP, where a ratio of 2.1 (1.7–2.9) was found.[58] Given the range of measurement techniques and diversity of biomes analyzed, the consistency of GPP:NPP estimates is remarkable. Although observed discrepancies between estimates are important avenues of future work, to date, there is no clear indication that GPP:NPP should have varied systematically over Earth's history. Therefore, we assume a fixed GPP:NPP to relate estimates of NPP to GPP through time.

than they do today.[65,66] Third, a gradual, rather than stepwise, rise of algae and terrestrial plants,[67] would increase the relative contribution of cyanobacteria to global productivity from the value estimated here. Fourth, if oxygenic photosynthesis originated more than half a billion years before the GOE,[21,22,25,68] then the contribution of cyanobacteria would be larger (Figure 1C; see also STAR Methods). Lastly, our discussion focuses on end-member scenarios, but we emphasize that intermediate scenarios are possible and that most favor a larger contribution of cyanobacteria to integrated productivity than our most probable trajectory.

How many cells have inhabited the Earth?

Accounting for estimates of cell density in Earth's modern surface and subsurface environments,[3,69–71] it is estimated that there is a standing stock of ~10^{30} living cells on Earth (see STAR Methods). Most of this population resides in the continental and marine subsurface,[70,71] followed by terrestrial soils and marine waters.[3,69] Considering the number of new cells produced annually, however, the order of the above deep-to-shallow relative abundances changes. Marine autotroph populations are the smallest, but their turnover times are shorter, with cyanobacteria likely being the shortest.[72] Subsurface populations are larger, but they turn over on much longer timescales.[69] Taking estimated turnover times into account, it can be deduced that annually ~10^{30} new cells come into existence (see STAR Methods), the majority of which are marine autotrophs and heterotrophs (the similarity with the standing stock estimate is fortuitous).

To translate insights gained from the modern biosphere throughout deep time, we first assume that the number of autotrophic and heterotrophic cells has always been proportional to primary productivity (autotrophs produce the biomass, heterotrophs use it as a substrate). Due to their rapid turnover,[72] cyanobacteria dominate the annual autotrophic cell population today, even though they account for only ≈10% of global primary productivity.[65] Hence, cyanobacteria have likely dominated the autotrophic cell population, at least since the GOE, and one can use the modern cyanobacterial productivity-abundance proportionality to translate the trajectory of cyanobacterial productivity into a census of the total number of autotrophs to have ever existed. A heterotroph-productivity proportionality is similarly used assuming that bacteria dominated heterotrophic cell numbers and that similar heterotrophic niches to today's existed throughout Earth's history. We find that within our uncertainty envelope and under all scenarios of productivity contributions, including an early emergence of oxygenic photosynthesis, that ~10^{39} (low-GOE) to ~10^{40} (high-GOE) cells have existed on Earth since the origin of life (see STAR Methods). Moreover, we find it is likely that autotrophic cells have dominated Earth's total cell population and that the most abundant taxon to have ever existed on Earth, in terms of cell number, is the cyanobacteria.

Cell population, random mutation, and selection

By piecing together estimates of global productivity through Earth's history, one can also constrain the breadth of random mutation throughout evolution and explore whether large shifts in productivity may have impacted evolutionary trajectories. We focus on cyanobacteria, as the most numerous group to have ever existed. The present-day number of cyanobacterial cells is ~10^{27}–10^{28}.[65] As cyanobacteria typically turn over on a timescale of days,[72] one arrives at an estimate of ~10^{29}–10^{30} annual replications of cyanobacteria.[73] Projected through the productivity trajectory presented here, this annual rate of cyanobacterial replication yields ~10^{39}–10^{40} replications ever (including uncertainty about primary productivity during

Table 1. Percentage of productivity contributed by the major primary producer groups

Scenario	Cyanobacteria	Algae	Plants	Other
High-productivity GOE	76	9	14	1
Low-productivity GOE	28	28	44	1
Maximal algal productivity	25	48	27	1
Maximal plant productivity	29	25	45	1
Maximal cyanobacterial productivity	36	37	27	1

The GOE high-productivity and low-productivity scenarios are based on our reference case (Data S3). The maximal contribution scenarios for cyanobacteria, algae, and land plants assume a low-productivity GOE with the emergence of these groups to dominance at the earliest extremes of existing estimates, respectively, and at the highest estimates of these groups' productivity, and assuming minimal contributions from other major groups, respectively (algae, land plants, or cyanobacteria). Details are provided in the STAR Methods, as are the results of other combinations of the uncertain timing and productivity estimates (Figures S3A–S3F).

the GOE). The characteristic current mutation rate in a wide range of bacteria is $\sim 10^{-10}$ mutations per base pair per replication,[74–78] and the genome size of the most common modern cyanobacteria (*Prochlorococcus*) is $\sim 10^6$ base pairs (1 Mb).[79] Therefore, in each cyanobacterial replication there are $\sim 10^{-4}$ mutation events. Thus, there have been $\sim 10^{35}$–10^{36} single-base-pair mutations in cyanobacteria through time. To illustrate the meaning of this value, as each base pair has 4 possible base options, $\sim 10^{35}$–10^{36} mutations cover all possible combinations of 5 base-pair mutations across the genome ($(4 \times 10^6)^5 \sim 10^{33}$), but not 6 ($(4 \times 10^6)^6 \sim 10^{39}$). All the mutations that ever occurred in cyanobacteria, therefore, only cover an infinitesimal fraction of the entire sequence space of possible 1 Mb genomes (which is $(4 \times 10^6)^{10^6} \sim 10^{6 \times 10^6}$).

The above calculations highlight the critical role of selective pressure in effective exploration of sequence space. If the rate at which life can explore sequence space is correlated to changes in biospheric productivity, then it may be necessary to consider changes to overall rates of adaptation and relative timing of major biological innovations. Decades of models and experiments quantifying the scaling between population size and evolutionary rate show substantial variation from a 1:1 relationship but support an overall positive trend.[80–85] This trend is often thought to experience diminishing returns with larger population size,[86] primarily due to clonal interference. However, sufficiently large populations or heterogeneous environments (as can be expected for global populations of cyanobacteria) can support the coexistence of multiple stable polymorphisms as discrete ecotypes.[87] Moreover, the main effect of horizontal gene transfer in such a population is not a change in the mutation rate but an increase in the fixation rate of favorable mutations, strengthening the link between population size and evolutionary rate. Evolutionary rates can, therefore, be assumed to vary substantially through time in association with large changes in the global rate of primary productivity such as the GOE (Figure 1A). The effect described here differs from the spikes in innovation associated with environmental changes such as the introduction of O_2 into biochemistry around the GOE, which is thought to have increased the diversity of metabolites and reactions among them.[88] Moreover, time-varying rates of evolution have implications for the calculation of molecular clocks, especially in the case of cyanobacteria and other lineages for which a large phylogenetic distance is made up of stem lineages unbroken by extant representatives.[89] In such cases, within-lineage variations of evolutionary rate are typically not accounted for in relaxed molecular clock models.[90]

As an example, it is informative to consider the effects of a simple rescaling of phylogenetic branch lengths of stem group cyanobacteria (i.e., the branches preceding the radiation of the extant crown group but postdating divergence of cyanobacteria from their closest surviving non-photosynthetic relatives) associated with the productivity increase over the GOE. Even when conservatively adopting a low-productivity GOE and a very weak scaling of adaptation rates with population size (1:100), our productivity trajectory and the associated increase in adaptation rate (i.e., decrease in branch length) should result in over 98% of molecular evolution in cyanobacteria occurring in the few hundred million years after the initiation of the GOE. This conservative scenario holds even if the first cyanobacteria originated well in advance of the GOE. This example emphasizes that using molecular clocks to estimate the timing of origin of taxa without deep, extensive calibrations or accounting for spikes of innovation associated with environmental change is even more imprecise than commonly recognized,[91] due to the productivity-dependent mapping of evolution onto actual geologic time. Although the lack of direct geologic evidence and associated uncertainty about the timing of the earliest events in the evolution of life makes it difficult to constrain the deepest branches of molecular clocks, an appropriate rescaling of these earliest branches to changes in productivity may render them negligible to the overall accumulation of evolutionary change. The absolute timing of the origin of cyanobacteria is clearly important for understanding the emergence of oxygenic photosynthesis. However, if over 99% of the evolution of this stem group occurred after the initiation of the GOE ≈ 2.4 Ga ago, then the amount of evolutionary innovation (e.g., number of mutations accumulated) may not differ meaningfully between a cyanobacterial origin at 3.0 versus 2.5 Ga ago.

Implications for the global carbon cycle

Estimating organic carbon burial throughout Earth history has canonically been achieved through stable carbon isotope mass balance (see STAR Methods). This framework must assume that $\delta^{13}C$ values of predominantly shallow marine carbonates are reliable recorders of the $\delta^{13}C$ values of marine dissolved inorganic carbon and that carbon isotopic discrimination between inorganic carbon and organic matter has been constant through time.[92] Combining these assumptions, it is argued[93] that over long timescales ≈20%–25% of the carbon entering the ocean-atmosphere from solid-Earth degassing has been buried as organic matter (f_{org} = 0.20–0.25; see also STAR Methods). If long-term solid-Earth degassing (the carbon source) has not significantly deviated from the modern value of ≈0.1 Gt C $year^{-1}$,[94,95] then this carbon isotope-based approach, when combined with our productivity trajectory, requires that the burial efficiency of organic carbon has decreased through time to maintain carbon mass balance (Figure 2). These inferred changes to the burial efficiency of organic carbon mirror changes

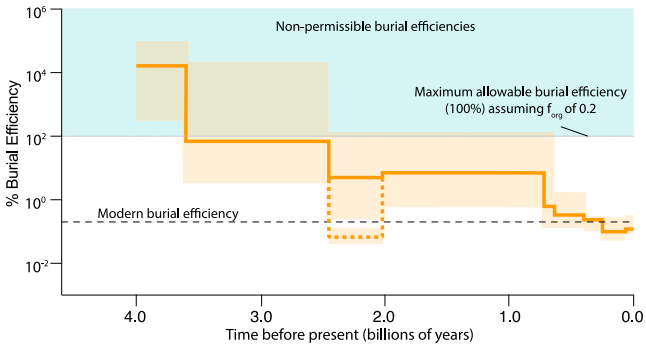

Figure 2. Calculated burial efficiency of organic matter through time

The dark orange line represents the most probable trajectory (given literature estimates) from Figure 1A, and the light orange envelope represents productivity uncertainties translated to burial efficiency uncertainties. The lower horizontal dotted line represents estimated modern burial efficiency (0.2%), and the light blue shaded region represents non-permissible burial efficiency >100%. Calculations were made assuming a constant degassing rate of 0.1 Gt C year^{-1} and that 20% of the degassed carbon is buried as organic matter (the rest as carbonate minerals; f_{org} = 0.2), as canonically inferred from the record of carbon isotope ratios in marine carbonate rocks. The dotted orange line represents an alternative burial efficiency trajectory in a scenario with an O_2 and productivity overshoot across Earth's GOE.

in primary productivity, and they may reflect the progressive oxygenation of Earth's surface environment (Figures 1A and 2). The implied negative feedback mechanism between O_2 levels and organic carbon burial, in which an increase in photosynthetic production of O_2 drives an increase in the rate of O_2 consumption by oxidation of organic matter, is thought to have been central in regulating atmospheric O_2.[96–99]

In combining carbon isotope-based models with our synthesis of existing productivity estimates during the Archean eon (4.0–2.5 Ga ago) one arrives at impossible burial efficiencies >100% (Figure 2). One way to reconcile this observation is that Archean productivity could not have been as low as is suggested in some studies[37,98,99] or that other key aspects of Earth's carbon cycle deviated significantly from present-day values, such as CO_2 degassing rates.[100] Alternatively, Archean $\delta^{13}C$ records and the carbon-cycle models used to interpret them may not faithfully represent global marine dissolved inorganic carbon or the Archean carbon cycle, respectively. For example, the $\delta^{13}C$ values of shallow marine carbonate sediments are commonly decoupled from the global marine dissolved inorganic carbon pool due to local carbon cycling and diagenetic processes.[101–104] Furthermore, examples of departures from the modern carbon cycle relevant to the Archean include significant organic synthesis through Fischer-Tropsch reactions,[105] preferential burial of isotopically light carbonate carbon,[102] or different carbon isotope discrimination into organic matter.[106] These and possibly other factors urge caution in making strong inferences about components of the early carbon cycle from our productivity trajectories.

The geologic future of primary productivity

The future of Earth's productivity trajectory is reliant on the availability of the ingredients of life and the environmental conditions necessary for it to thrive. Stellar evolution imposes a trade-off between these two requirements. As the Sun ages, progressively more hydrogen will combine into helium, the Sun's core will become denser, the pace of nuclear reactions will increase, and more photons will hit Earth's surface per unit time.[107] It is thought that this solar brightening will be compensated by a decrease in the atmospheric concentration of CO_2 through the stabilizing effect of the silicate weathering feedback.[108] As the Sun continues to brighten, CO_2 will drop to levels too low for the activity of the enzyme responsible for the majority of photosynthetic carbon fixation (D-ribulose 1,5-bisphosphate carboxylase/oxygenase; rubisco). Projecting current models of future climate, it is estimated that CO_2 limitation will cause plants to die off within $\sim 10^9$ years.[109–112] Once this CO_2 threshold is reached, primary productivity in the ocean will persist, as marine autotrophs can operate under CO_2 concentrations lower than their terrestrial counterparts.[113]

Irrespective of the exact timing of CO_2 limitation of primary producers, further into the future solar brightening will lead to marine temperatures that no longer permit the synthesis and maintenance of biomolecular machinery. Precluding the possibility of major cataclysm shortening the habitable lifetime of Earth, or biological innovation or geoengineering lengthening it, a runaway greenhouse is predicted within $\approx 2 \times 10^9$ years.[111,112,114,115] If one assumes that future primary productivity is similar in makeup to the modern, it can be inferred that we are likely living close to the 50% mark of the total carbon that will ever be fixed by Earth's biosphere. This inference further implies that it is unlikely that Earth's biosphere will ever grow beyond a time-integrated $\sim 10^{41}$ cells across the planet's entire habitable lifetime. Although the amount of time left for the biosphere is less than the time life has existed on Earth, the extension of today's relatively high rates of primary productivity will likely squeeze more life into less time.

STAR★METHODS

Detailed methods are provided in the online version of this paper and include the following:

- KEY RESOURCES TABLE
- RESOURCE AVAILABILITY
  - Lead contact
  - Materials availability
  - Data and code availability
- EXPERIMENTAL MODEL AND SUBJECT DETAILS
- METHOD DETAILS
  - Time bins
  - Literature estimates
  - Earth's Great Oxidation Event
  - Integrating productivity estimates
  - Contributions to productivity through time
  - Estimating the historically integrated cell population of the Earth
  - Carbon cycling and carbon mass balance
- QUANTIFICATION AND STATISTICAL ANALYSIS

SUPPLEMENTAL INFORMATION

Supplemental information can be found online at https://doi.org/10.1016/j.cub.2023.09.040.

ACKNOWLEDGMENTS

The authors would like to sincerely thank Boswell Wing, Kevin Sutherland, John Raven, and Avi Flamholz for constructive input on this manuscript, as well as three anonymous reviewers who also helped to improve this work. This project was funded through a Zuckerman STEM Leadership Postdoctoral Fellowship to P.W.C. and the Woods Hole Oceanographic Institution Postdoctoral Scholar Program.

AUTHOR CONTRIBUTIONS

Conceptualization, P.W.C., I.H., and R.M.; methodology and formal analysis, all authors; visualization, P.W.C., I.H., R.M., and Y.M.B.O.; data curation, P.W.C. and I.H.; funding acquisition, P.W.C.; writing of original and revised drafts, all authors.

DECLARATION OF INTERESTS

The authors declare no competing interests.

Received: July 28, 2023
Revised: September 11, 2023
Accepted: September 18, 2023
Published: October 11, 2023

REFERENCES

1. Geider, R.J., Delucia, E.H., Falkowski, P.G., Finzi, A.C., Grime, J.P., Grace, J., Kana, T.M., La Roche, J., Long, S.P., Osborne, B.A., et al. (2001). Primary productivity of planet earth: biological determinants and physical constraints in terrestrial and aquatic habitats. Glob. Change Biol. *7*, 849–882. https://doi.org/10.1046/j.1365-2486.2001.00448.x.
2. Redfield, A., Ketchum, B., and Richards, F. (1963). The influence of organisms on the composition of seawater. The Sea *2*, 26–77.
3. Bar-On, Y.M., Phillips, R., and Milo, R. (2018). The biomass distribution on earth. Proc. Natl. Acad. Sci. USA *115*, 6506–6511. https://doi.org/10.1073/pnas.1711842115.
4. Holland, H.D. (2006). The oxygenation of the atmosphere and oceans. Philos. Trans. R. Soc. Lond. B Biol. Sci. *361*, 903–915. https://doi.org/10.1098/rstb.2006.1838.
5. Field, C.B., Behrenfeld, M.J., Randerson, J.T., and Falkowski, P. (1998). Primary production of the biosphere: integrating terrestrial and oceanic components. Science *281*, 237–240. https://doi.org/10.1126/science.281.5374.237.
6. Yang, J.-W., Brandon, M., Landais, A., Duchamp-Alphonse, S., Blunier, T., Prié, F., and Extier, T. (2022). Global biosphere primary productivity changes during the past eight glacial cycles. Science *375*, 1145–1151. https://doi.org/10.1126/science.abj8826.
7. Lenton, T.M., Dahl, T.W., Daines, S.J., Mills, B.J.W., Ozaki, K., Saltzman, M.R., and Porada, P. (2016). Earliest land plants created modern levels of atmospheric oxygen. Proc. Natl. Acad. Sci. USA *113*, 9704–9709. https://doi.org/10.1073/pnas.1604787113.
8. Crockford, P.W., Hayles, J.A., Bao, H., Planavsky, N.J., Bekker, A., Fralick, P.W., Halverson, G.P., Bui, T.H., Peng, Y., and Wing, B.A. (2018). Triple oxygen isotope evidence for limited mid-Proterozoic primary productivity. Nature *559*, 613–616. https://doi.org/10.1038/s41586-018-0349-y.
9. Longhurst, A., Sathyendranath, S., Platt, T., and Caverhill, C. (1995). An estimate of global primary production in the ocean from satellite radiometer data. J. Plankton Res. *17*, 1245–1271.
10. Norton, A.J., Rayner, P.J., Koffi, E.N., Scholze, M., Silver, J.D., and Wang, Y.-P. (2019). Estimating global gross primary productivity using chlorophyll fluorescence and a data assimilation system with the Bethy-scope model. Biogeosciences *16*, 3069–3093. https://doi.org/10.5194/bg-16-3069-2019.
11. Huang, Y., Nicholson, D., Huang, B., and Cassar, N. (2021). Global estimates of marine gross primary production based on machine learning upscaling of field observations. Glob. Biogeochem. Cyc. *35*, GB006718, https://doi.org/10.1029/2020GB006718.
12. Farquhar, J., Bao, H., and Thiemens, M. (2000). Atmospheric influence of earth's earliest sulfur cycle. Science *289*, 756–759. https://doi.org/10.1126/science.289.5480.756.
13. Crockford, P.W., Kunzmann, M., Bekker, A., Hayles, J., Bao, H., Halverson, G.P., Peng, Y., Bui, T.H., Cox, G.M., Gibson, T.M., et al. (2019). Claypool continued: extending the isotopic record of sedimentary sulfate. Chem. Geol. *513*, 200–225. https://doi.org/10.1016/j.chemgeo.2019.02.030.
14. Johnson, J.E., Gerpheide, A., Lamb, M.P., and Fischer, W.W. (2014). O2 constraints from Paleoproterozoic detrital pyrite and uraninite. GSA Bull. *126*, 813–830. https://doi.org/10.1130/B30949.1.
15. Luo, G., Ono, S., Beukes, N.J., Wang, D.T., Xie, S., and Summons, R.E. (2016). Rapid oxygenation of earth's atmosphere 2.33 billion years ago. Sci. Adv. *2*, e1600134, https://doi.org/10.1126/sciadv.1600134.
16. Gumsley, A.P., Chamberlain, K.R., Bleeker, W., Söderlund, U., de Kock, M.O., Larsson, E.R., and Bekker, A. (2017). Timing and tempo of the great oxidation event. Proc. Natl. Acad. Sci. USA *114*, 1811–1816. https://doi.org/10.1073/pnas.1608824114.
17. Warke, M.R., Di Rocco, T., Zerkle, A.L., Lepland, A., Prave, A.R., Martin, A.P., Ueno, Y., Condon, D.J., and Claire, M.W. (2020). The great oxidation event preceded a Paleoproterozoic "snowball earth". Proc. Natl. Acad. Sci. USA *117*, 13314–13320. https://doi.org/10.1073/pnas.2003090117.
18. Brocks, J.J., Jarrett, A.J.M., Sirantoine, E., Hallmann, C., Hoshino, Y., and Liyanage, T. (2017). The rise of algae in Cryogenian oceans and the emergence of animals. Nature *548*, 578–581. https://doi.org/10.1038/nature23457.
19. Isson, T.T., Love, G.D., Dupont, C.L., Reinhard, C.T., Zumberge, A.J., Asael, D., Gueguen, B., McCrow, J., Gill, B.C., Owens, J., et al. (2018). Tracking the rise of eukaryotes to ecological dominance with zinc isotopes. Geobiology *16*, 341–352. https://doi.org/10.1111/gbi.12289.
20. Zumberge, J.A., Rocher, D., and Love, G.D. (2020). Free and kerogen-bound biomarkers from Late Tonian sedimentary rocks record abundant eukaryotes in mid-Neoproterozoic marine communities. Geobiology *18*, 326–347. https://doi.org/10.1111/gbi.12378.
21. Planavsky, N.J., Asael, D., Hofmann, A., Reinhard, C.T., Lalonde, S.V., Knudsen, A., Wang, X., Ossa Ossa, F., Pecoits, E., Smith, A.J.B., et al. (2014). Evidence for oxygenic photosynthesis half a billion years before the great oxidation event. Nature Geosci. *7*, 283–286. https://doi.org/10.1038/ngeo2122.
22. Jabłonska, J., and Tawfik, D.S. (2021). The evolution of oxygen-utilizing enzymes suggests early biosphere oxygenation. Nat. Ecol. Evol. *5*, 442–448. https://doi.org/10.1038/s41559-020-01386-9.
23. Goldblatt, C., Lenton, T.M., and Watson, A.J. (2006). Bistability of atmospheric oxygen and the great oxidation. Nature *443*, 683–686. https://doi.org/10.1038/nature05169.
24. Olson, S.L., Kump, L.R., and Kasting, J.F. (2013). Quantifying the areal extent and dissolved oxygen concentrations of archean oxygen oases. Chem. Geol. *362*, 35–43. https://doi.org/10.1016/j.chemgeo.2013.08.012.
25. Ostrander, C.M., Johnson, A.C., and Anbar, A.D. (2021). Earth's first redox revolution. Annu. Rev. Earth Planet. Sci. *49*, 337–366. https://doi.org/10.1146/annurev-earth-072020-055249.
26. Eckford-Soper, L.K., Andersen, K.H., Hansen, T.F., and Canfield, D.E. (2022). A case for an active eukaryotic marine biosphere during the Proterozoic era. Proc. Natl. Acad. Sci. USA *119*, e2122042119, https://doi.org/10.1073/pnas.2122042119.
27. Gensel, P.G., and Edwards, D. (2001). Plants Invade the Land (Columbia University Press).
28. Stein, W.E., Mannolini, F., Hernick, L.V., Landing, E., and Berry, C.M. (2007). Giant cladoxylopsid trees resolve the enigma of the earth's

earliest forest stumps at gilboa. Nature *446*, 904–907. https://doi.org/10.1038/nature05705.

29. Donoghue, P.C.J., Harrison, C.J., Paps, J., and Schneider, H. (2021). The evolutionary emergence of land plants. Curr. Biol. *31*, R1281–R1298. https://doi.org/10.1016/j.cub.2021.07.038.
30. Kirschvink, J.L., Gaidos, E.J., Bertani, L.E., Beukes, N.J., Gutzmer, J., Maepa, L.N., and Steinberger, R.E. (2000). Paleoproterozoic snowball earth: extreme climatic and geochemical global change and its biological consequences. Proc. Natl. Acad. Sci. USA *97*, 1400–1405. https://doi.org/10.1073/pnas.97.4.1400.
31. Hoffman, P.F., Abbot, D.S., Ashkenazy, Y., Benn, D.I., Brocks, J.J., Cohen, P.A., Cox, G.M., Creveling, J.R., Donnadieu, Y., Erwin, D.H., et al. (2017). Snowball earth climate dynamics and Cryogenian geology-geobiology. Sci. Adv. *3*, e1600983, https://doi.org/10.1126/sciadv.1600983.
32. Bambach, R.K. (2006). Phanerozoic biodiversity mass extinctions. Annu. Rev. Earth Planet. Sci. *34*, 127–155. https://doi.org/10.1146/annurev.earth.33.092203.122654.
33. Erwin, D.H. (2015). Extinction: How Life on Earth Nearly Ended 250 Million Years Ago-Updated Edition*37* (Princeton University Press).
34. Beerling, D.J. (1999). Quantitative estimates of changes in marine and terrestrial primary productivity over the past 300 million years. Proc. R. Soc. Lond. B *266*, 1821–1827. https://doi.org/10.1098/rspb.1999.0852.
35. Blunier, T., Bender, M.L., Barnett, B., and Von Fischer, J.C. (2012). Planetary fertility during the past 400 ka based on the triple isotope composition of o 2 in trapped gases from the vostok ice core. Clim. Past *8*, 1509–1526. https://doi.org/10.5194/cp-8-1509-2012.
36. Canfield, D.E., Rosing, M.T., and Bjerrum, C. (2006). Early anaerobic metabolisms discussion 1835. Philos. Trans. R. Soc. Lond. B Biol. Sci. *361*. 1819-34. https://doi.org/10.1098/rstb.2006.1906.
37. Daines, S.J., and Lenton, T.M. (2016). The effect of widespread early aerobic marine ecosystems on methane cycling and the great oxidation. Earth Planet. Sci. Lett. *434*, 42–51. https://doi.org/10.1016/j.epsl.2015.11.021.
38. Derry, L.A. (2015). Causes and consequences of mid-Proterozoic anoxia. Geophys. Res. Lett. *42*, 8538–8546. https://doi.org/10.1002/2015GL065333.
39. De Marais, D.J. (2000). Evolution. When did photosynthesis emerge on earth? Science *289*, 1703–1705. https://doi.org/10.1126/science.289.5485.1703.
40. Edwards, D., Cherns, L., and Raven, J.A. (2015). Could land-based early photosynthesizing ecosystems have bioengineered the planet in mid-Palaeozoic times? Palaeontology *58*, 803–837. https://doi.org/10.1111/pala.12187.
41. Hao, J., Knoll, A.H., Huang, F., Schieber, J., Hazen, R.M., and Daniel, I. (2020). Cycling phosphorus on the archean earth: Part ii. phosphorus limitation on primary production in archean ecosystems. Geochim. Cosmochim. Acta *280*, 360–377. https://doi.org/10.1016/j.gca.2020.04.005.
42. Hodgskiss, M.S.W., Crockford, P.W., Peng, Y., Wing, B.A., and Horner, T.J. (2019). A productivity collapse to end earth's great oxidation. Proc. Natl. Acad. Sci. USA *116*, 17207–17212. https://doi.org/10.1073/pnas.1900325116.
43. Sharoni, S., and Halevy, I. (2023). Rates of seafloor and continental weathering govern Phanerozoic marine phosphate levels. Nat. Geosci. *16*, 75–81. https://doi.org/10.1038/s41561-022-01075-1.
44. Sleep, N.H., and Bird, D.K. (2007). Niches of the pre-photosynthetic biosphere and geologic preservation of earth's earliest ecology. Geobiology *5*, 101–117. https://doi.org/10.1111/j.1472-4669.2007.00105.x.
45. Wing, B.A. (2013). A cold, hard look at ancient oxygen. Proc. Natl. Acad. Sci. USA *110*, 14514–14515. https://doi.org/10.1073/pnas.1313197110.
46. Ward, L.M., Rasmussen, B., and Fischer, W.W. (2019). Primary productivity was limited by electron donors prior to the advent of oxygenic photosynthesis. J. Geophys. Res.: Biogeosci. *124*, 211–226. https://doi.org/10.1073/pnas.1313197110.
47. Sauterey, B., Charnay, B., Affholder, A., Mazevet, S., and Ferrière, R. (2020). Co-evolution of primitive' methane-cycling ecosystems and early earth's atmosphere and climate. Nat. Commun. *11*, 2705, https://doi.org/10.1038/s41467-020-16374-7.
48. Planavsky, N.J., Fakhraee, M., Bolton, E.W., Reinhard, C.T., Isson, T.T., Zhang, S., and Mills, B.J.W. (2022). On carbon burial and net primary production through earth's history. Am. J. Sci. *322*, 413–460. https://doi.org/10.2475/03.2022.01.
49. Kharecha, P., Kasting, J., and Siefert, J. (2005). A coupled atmosphere–ecosystem model of the early archean earth. Geobiology *3*, 53–76. https://doi.org/10.1111/j.1472-4669.2005.00049.x.
50. Laakso, T.A., and Schrag, D.P. (2017). A theory of atmospheric oxygen. Geobiology *15*, 366–384. https://doi.org/10.1111/gbi.12230.
51. Laakso, T.A., and Schrag, D.P. (2019). A small marine biosphere in the Proterozoic. Geobiology *17*, 161–171. https://doi.org/10.1111/gbi.12323.
52. Holland, H.D. (2002). Volcanic gases, black smokers, and the great oxidation event. Geochim. Cosmochim. Acta *66*, 3811–3826. https://doi.org/10.1016/S0016-7037(02)00950-X.
53. Bekker, A., and Holland, H.D. (2012). Oxygen overshoot and recovery during the Early Paleoproterozoic. Earth Planet. Sci. Lett. *317–318*, 295–304. https://doi.org/10.1016/j.epsl.2011.12.012.
54. Sanz-Martín, M., Vernet, M., Cape, M.R., Mesa, E., Delgado-Huertas, A., Reigstad, M., Wassmann, P., and Duarte, C.M. (2019). Relationship between carbon-and oxygen-based primary productivity in the arctic ocean, Svalbard Archipelago. Front. Mar. Sci. *6*, 468, https://doi.org/10.3389/fmars.2019.00468.
55. Sigman, D.M., and Hain, M.P. (2012). The Biological Productivity of the Ocean. Nat. Edu. Knowl. *3*, 1–16.
56. Raven, J.A. (2009). Contributions of anoxygenic and oxygenic phototrophy and chemolithotrophy to carbon and oxygen fluxes in aquatic environments. Aquat. Microb. Ecol. *56*, 177–192. https://doi.org/10.3354/ame01315.
57. Juranek, L.W., and Quay, P.D. (2013). Using triple isotopes of dissolved oxygen to evaluate global marine productivity. Annu. Rev. Mar. Sci. *5*, 503–524. https://doi.org/10.1146/annurev-marine-121211-172430.
58. Collalti, A., and Prentice, I.C. (2019). Is npp proportional to gpp? waring's hypothesis 20 years on. Tree Physiol. *39*, 1473–1483.
59. Marty, B. (2012). The origins and concentrations of water, carbon, nitrogen and noble gases on earth. Earth Planet. Sci. Lett. *313–314*, 56–66. https://doi.org/10.1016/j.epsl.2011.10.040.
60. Hirschmann, M.M. (2023). The deep Earth oxygen cycle: mass balance considerations on the origin and evolution of mantle and surface oxidative reservoirs. Earth Planet. Sci. Lett. *619*, 118311, https://doi.org/10.1016/j.epsl.2023.118311.
61. Rasmussen, B., Bekker, A., and Fletcher, I.R. (2013). Correlation of Paleoproterozoic glaciations based on u–pb zircon ages for tuff beds in the transvaal and Huronian supergroups. Earth Planet. Sci. *382*, 173–180. https://doi.org/10.1016/j.epsl.2013.08.037.
62. Van de Peer, Y., Mizrachi, E., and Marchal, K. (2017). The evolutionary significance of polyploidy. Nat. Rev. Genet. *18*, 411–424. https://doi.org/10.1038/nrg.2017.26.
63. Del Cortona, A., Jackson, C.J., Bucchini, F., Van Bel, M., D'hondt, S., Skaloud, P., Delwiche, C.F., Knoll, A.H., Raven, J.A., and Verbruggen, H. (2020). Neoproterozoic origin and multiple transitions to macroscopic growth in green seaweeds. Proc. Natl. Acad. Sci. USA *117*, 2551–2559. https://doi.org/10.1073/pnas.19100601.
64. Jablonski, D. (2001). Lessons from the past: evolutionary impacts of mass extinctions. Proc. Natl. Acad. Sci. USA *98*, 5393–5398. https://doi.org/10.1073/pnas.101092598.
65. Flombaum, P., Gallegos, J.L., Gordillo, R.A., Rincón, J., Zabala, L.L., Jiao, N., Karl, D.M., Li, W.K.W., Lomas, M.W., Veneziano, D., et al.

(2013). Present and future global distributions of the marine cyanobacteria Prochlorococcus and Synechococcus. Proc. Natl. Acad. Sci. USA *110*, 9824–9829. https://doi.org/10.1073/pnas.1307701110.

66. Middelburg, J.J. (2019). Marine carbon biogeochemistry: A primer for earth system scientists (Springer Nature journals unify their policy to encourage preprint sharing. Nature *569*, 307.
67. Morris, J.L., Puttick, M.N., Clark, J.W., Edwards, D., Kenrick, P., Pressel, S., Wellman, C.H., Yang, Z., Schneider, H., and Donoghue, P.C.J. (2018). The timescale of early land plant evolution. Proc. Natl. Acad. Sci. USA *115*, E2274–E2283. https://doi.org/10.1073/pnas.1719588115.
68. Johnson, A.C., Ostrander, C.M., Romaniello, S.J., Reinhard, C.T., Greaney, A.T., Lyons, T.W., and Anbar, A.D. (2021). Reconciling evidence of oxidative weathering and atmospheric anoxia on archean earth. Sci. Adv. *7*, eabj0108, https://doi.org/10.1126/sciadv.abj0108.
69. Whitman, W.B., Coleman, D.C., and Wiebe, W.J. (1998). Prokaryotes: the unseen majority. Proc. Natl. Acad. Sci. USA *95*, 6578–6583. https://doi.org/10.1073/pnas.95.12.6578.
70. Parkes, R.J., Cragg, B., Roussel, E., Webster, G., Weightman, A., and Sass, H. (2014). A review of prokaryotic populations and processes in sub-seafloor sediments, including biosphere: geosphere interactions. Mar. Geol. *352*, 409–425. https://doi.org/10.1016/j.margeo.2014.02.009.
71. Magnabosco, C., Lin, L.-H., Dong, H., Bomberg, M., Ghiorse, W., Stan-Lotter, H., Pedersen, K., Kieft, T.L., van Heerden, E., and Onstott, T.C. (2018). The biomass and biodiversity of the continental subsurface. Nature Geosci. *11*, 707–717. https://doi.org/10.1038/s41561-018-0221-6.
72. Zubkov, M.V. (2014). Faster growth of the major prokaryotic versus eukaryotic co 2 fixers in the oligotrophic ocean. Nat. Commun. *5*, 3776, https://doi.org/10.1038/ncomms4776.
73. Phillips, R., and Milo, R. (2009). A feeling for the numbers in biology. Proc. Natl. Acad. Sci. USA *106*, 21465–21471. https://doi.org/10.1073/pnas.0907732106.
74. Wielgoss, S., Barrick, J.E., Tenaillon, O., Cruveiller, S., Chane-Woon-Ming, B., Médigue, C., Lenski, R.E., and Schneider, D. (2011). Mutation rate inferred from synonymous substitutions in a long-term evolution experiment with Escherichia coli: Genes— Genomes. Genetics *1*, 183–186. https://doi.org/10.1534/g3.111.000406.
75. Imhof, M., and Schlotterer, C. (2001). Fitness effects of advantageous mutations in evolving escherichiä coli populations. Proc. Natl. Acad. Sci. USA *98*, 1113–1117. https://doi.org/10.1073/pnas.98.3.1113.
76. Denef, V.J., and Banfield, J.F. (2012). In situ evolutionary rate measurements show ecological success of recently emerged bacterial hybrids. Science *336*, 462–466. https://doi.org/10.1126/science.1218389.
77. Drake, J.W., Charlesworth, B., Charlesworth, D., and Crow, J.F. (1998). Rates of spontaneous mutation. Genetics *148*, 1667–1686. https://doi.org/10.1093/genetics/148.4.1667.
78. Lee, H., Popodi, E., Tang, H., and Foster, P.L. (2012). Rate and molecular spectrum of spontaneous mutations in the bacterium Escherichia coli as determined by whole-genome sequencing. Proc. Natl. Acad. Sci. USA *109*, E2774–E2783. https://doi.org/10.1073/pnas.1210309109.
79. Nordberg, H., Cantor, M., Dusheyko, S., Hua, S., Poliakov, A., Shabalov, I., Smirnova, T., Grigoriev, I.V., and Dubchak, I. (2014). The genome portal of the Department of Energy Joint Genome Institute: 2014 updates. Nucleic Acids Res. *42*, D26–D31.
80. Chavhan, Y. (2019). The Effects of Population Size on Adaptation and Trade-offs: Insights from Experimental Evolution with Escherichia coli and Individual-based Models. Ph.D. thesis.
81. Elena, S.F., and Lenski, R.E. (2003). Evolution experiments with microorganisms: the dynamics and genetic bases of adaptation. Nat. Rev. Genet. *4*, 457–469. https://doi.org/10.1038/nrg1088.
82. Wilke, C.O. (2004). The speed of adaptation in large asexual populations. Genetics *167*, 2045–2053. https://doi.org/10.1534/genetics.104.027136.
83. Szendro, I.G., Franke, J., de Visser, J.A.G., and Krug, J. (2013). Predictability of evolution depends nonmonotonically on population size. Proc. Natl. Acad. Sci. USA *110*, 571–576. https://doi.org/10.1073/pnas.1213613110.
84. de Visser, J.A.G., and Rozen, D.E. (2005). Limits to adaptation in asexual populations. J. Evol. Biol. *18*, 779–788. https://doi.org/10.1111/j.1420-9101.2005.00879.x.
85. Vahdati, A.R., and Wagner, A. (2018). Population size affects adaptation in complex ways: simulations on empirical adaptive landscapes. Evol. Biol. *45*, 156–169. https://doi.org/10.1007/s11692-017-9440-9.
86. Miralles, R., Moya, A., and Elena, S.F. (2000). Diminishing returns of population size in the rate of rna virus adaptation. J. Virol. *74*, 3566–3571. https://doi.org/10.1128/jvi.74.8.3566-3571.2000.
87. Hindré, T., Knibbe, C., Beslon, G., and Schneider, D. (2012). New insights into bacterial adaptation' through in vivo and in silico experimental evolution. Nat. Rev. Microbiol. *10*, 352–365. https://doi.org/10.1038/nrmicro2750.
88. David, L.A., and Alm, E.J. (2011). Rapid evolutionary innovation during an archaean genetic expansion. Nature *469*, 93–96. https://doi.org/10.1038/nature09649.
89. Ward, L.M., and Shih, P.M. (2019). The evolution and productivity of carbon fixation pathways in response to changes in oxygen concentration over geological time. Free Radic. Biol. Med. *140*, 188–199. https://doi.org/10.1016/j.freeradbiomed.2019.01.049.
90. Ho, S.Y., and Duchêne, S. (2014). Molecular-clock methods for estimating evolutionary rates and^ timescales. Mol. Ecol. *23*, 5947–5965. https://doi.org/10.1111/mec.12953.
91. Graur, D., and Martin, W. (2004). Reading the entrails of chickens: molecular timescales of evolution and the illusion of precision. Trends Genet. *20*, 80–86. https://doi.org/10.1016/j.tig.2003.12.003.
92. Hurley, S.J., Wing, B.A., Jasper, C.E., Hill, N.C., and Cameron, J.C. (2021). Carbon isotope evidence for the global physiology of Proterozoic cyanobacteria. Sci. Adv. *7*, eabc8998, https://doi.org/10.1126/sciadv.abc8998.
93. Krissansen-Totton, J., Buick, R., and Catling, D.C. (2015). A statistical analysis of the carbon isotope record from the archean to Phanerozoic and implications for the rise of oxygen. Am. J. Sci. *315*, 275–316. https://doi.org/10.2475/04.2015.01.
94. Sleep, N.H., and Zahnle, K. (2001). Carbon dioxide cycling and implications for climate on ancient earth. J. Geophys. Res. *106*, 1373–1399. https://doi.org/10.1029/2000JE001247.
95. Korenaga, J. (2006). Archean geodynamics and the thermal evolution of earth. Geophys. Monograph. Am. Geophys. Union *164*, 7–32.
96. Hayes, J.M., and Waldbauer, J.R. (2006). The carbon cycle and associated redox processes through time. Philos. Trans. R. Soc. Lond. B Biol. Sci. *361*, 931–950. https://doi.org/10.1098/rstb.2006.1840.
97. Daines, S.J., Mills, B.J., and Lenton, T.M. (2017). Atmospheric oxygen regulation at low Proterozoic levels by incomplete oxidative weathering of sedimentary organic carbon. Nat. Commun. *8*, 14379, https://doi.org/10.1038/ncomms14379.
98. Kipp, M.A., Krissansen-Totton, J., and Catling, D.C. (2021). High organic burial efficiency is required to explain mass balance in earth's early carbon cycle. Glob. Biogeochem. Cyc. *35*, https://doi.org/10.1029/2020GB006707.
99. Krissansen-Totton, J., Kipp, M.A., and Catling, D.C. (2021). Carbon cycle inverse modeling suggests large changes in fractional organic burial are consistent with the carbon isotope record and may have contributed to the rise of oxygen. Geobiology *19*, 342–363. https://doi.org/10.1111/gbi.12440.
100. Lee, C.-T.A., Yeung, L.Y., Mckenzie, N.R., Yokoyama, Y., Ozaki, K., and Lenardic, A. (2016). Two-step rise of atmospheric oxygen linked to the growth of continents. Nat. Geosci. *9*, 417–424. https://doi.org/10.1038/ngeo2707.
101. Swart, P.K. (2008). Global synchronous changes in the carbon isotopic composition of carbonate sediments unrelated to changes in the global

carbon cycle. Proc. Natl. Acad. Sci. USA *105*, 13741–13745. https://doi.org/10.1073/pnas.0802841105.

102. Geyman, E.C., and Maloof, A.C. (2019). A diurnal carbon engine explains 13c-enriched carbonates without increasing the global production of oxygen. Proc. Natl. Acad. Sci. USA *116*, 24433–24439. https://doi.org/10.1073/pnas.1908783116.
103. Higgins, J.A., Blättler, C.L., Lundstrom, E.A., Santiago-Ramos, D.P., Akhtar, A.A., Crüger Ahm, A.S., Bialik, O., Holmden, C., Bradbury, H., Murray, S.T., et al. (2018). Mineralogy, early marine diagenesis, and the chemistry of shallow-water carbonate sediments. Geochim. Cosmochim. Acta *220*, 512–534. https://doi.org/10.1016/j.gca.2017.09.046.
104. Crockford, P.W., Kunzmann, M., Blättler, C.L., Kalderon-Asael, B., Murphy, J.G., Ahm, A.S., Sharoni, S., Halverson, G.P., Planavsky, N.J., Halevy, I., et al. (2021). Reconstructing Neoproterozoic seawater chemistry from early diagenetic dolomite. Geology *49*, 442–446. https://doi.org/10.1130/G48213.1.
105. Brasier, M.D., Green, O.R., Jephcoat, A.P., Kleppe, A.K., Van Kranendonk, M.J., Lindsay, J.F., Steele, A., and Grassineau, N.V. (2002). Questioning the evidence for earth's oldest fossils. Nature *416*, 76–81.
106. Wang, R.Z., Nichols, R.J., Liu, A.K., Flamholz, A.I., Artier, J., Banda, D.M., Savage, D.F., Eiler, J.M., Shih, P.M., and Fischer, W.W. (2023). Carbon isotope fractionation by an ancestral RuBisCO suggests that biological proxies for CO2 through geologic time should be reevaluated. Proc. Natl. Acad. Sci. USA *120*, e2300466120, https://doi.org/10.1073/pnas.2300466120.
107. Gough, D.O. (1981). Solar interior structure and luminosity variations. Sol. Phys. *74*, 21–34.
108. Walker, J.C.G., Hays, P.B., and Kasting, J.F. (1981). A negative feedback mechanism for the long-term stabilization of earth's surface temperature. J. Geophys. Res. *86*, 9776–9782. https://doi.org/10.1029/JC086iC10p09776.
109. Lovelock, J.E., and Whitfield, M. (1982). Life span of the biosphere. Nature *296*, 561–563. https://doi.org/10.1038/296561a0.
110. Lenton, T.M., and von Bloh, W. (2001). Biotic feedback extends the life span of the biosphere. Geophys. Res. Lett. *28*, 1715–1718. https://doi.org/10.1029/2000GL012198.
111. Caldeira, K., and Kasting, J.F. (1992). The life span of the biosphere revisited. Nature *360*, 721–723. https://doi.org/10.1038/360721a0.
112. Mello, F., and Friaça, A.C.S. (2020). The end of life on earth is not the end of the world: converging to an estimate of life span of the biosphere? Int. J. Astrobiol. *19*, 25–42. https://doi.org/10.1017/S1473550419000120.
113. Miller, A.G., Turpin, D.H., and Canvin, D.T. (1984). Growth and photosynthesis of the cyanobacterium Synechococcus leopoliensis in hco3-limited chemostats. Plant Physiol. *75*, 1064–1070. https://doi.org/10.1104/pp.75.4.1064.
114. Franck, S., Block, A., Von Bloh, W., Bounama, C., Schellnhuber, H.J., and Svirezhev, Y. (2000). Reduction of biosphere life span as a consequence of geodynamics. Tellus B *52*, 94–107. https://doi.org/10.1034/j.1600-0889.2000.00898.x.
115. Ozaki, K., and Reinhard, C.T. (2021). The future lifespan of earth's oxygenated atmosphere. Nat. Geosci. *14*, 138–142. https://doi.org/10.1038/s41561-021-00693-5.
116. Cao, X., and Bao, H. (2013). Dynamic model constraints on oxygen-17 depletion in atmospheric o2 after a snowball earth. Proc. Natl. Acad. Sci. USA *110*, 14546–14550. https://doi.org/10.1073/pnas.1302972110.
117. Eickmann, B., Hofmann, A., Wille, M., Bui, T.H., Wing, B.A., and Schoenberg, R. (2018). Isotopic evidence for oxygenated mesoarchaean shallow oceans. Nature Geosci. *11*, 133–138. https://doi.org/10.1038/s41561-017-0036-x.
118. Falkowski, P.G., Katz, M.E., Knoll, A.H., Quigg, A., Raven, J.A., Schofield, O., and Taylor, F.J.R. (2004). The evolution of modern eukaryotic phytoplankton. Science *305*, 354–360. https://doi.org/10.1126/science.1095964.
119. Liu, P., Liu, J., Ji, A., Reinhard, C.T., Planavsky, N.J., Babikov, D., Najjar, R.G., and Kasting, J.F. (2021). Triple oxygen isotope constraints on atmospheric o2 and biological productivity during the mid-Proterozoic. Proc. Natl. Acad. Sci. USA *118*, e2105074118, https://doi.org/10.1073/pnas.2105074118.
120. Balci, N., Shanks, W.C., III, Mayer, B., and Mandernack, K.W. (2007). Oxygen and sulfur isotope systematics of sulfate produced by bacterial and abiotic oxidation of pyrite. Geochim. Cosmochim. Acta *71*, 3796–3811. https://doi.org/10.1016/j.gca.2007.04.017.
121. Pack, A., Höweling, A., Hezel, D.C., Stefanak, M.T., Beck, A.K., Peters, S.T.M., SenGupta, S., Herwartz, D., and Folco, L. (2017). Tracing the oxygen isotope composition of the upper earth's atmosphere using cosmic spherules. Nat. Commun. *8*, 15702, https://doi.org/10.1038/ncomms15702.
122. Waldeck, A.R., Cowie, B.R., Bertran, E., Wing, B.A., Halevy, I., and Johnston, D.T. (2019). Deciphering the atmospheric signal in marine sulfate oxygen isotope composition. Earth Planet. Sci. Lett. *522*, 12–19. https://doi.org/10.1016/j.epsl.2019.06.013.
123. Killingsworth, B.A., Bao, H., and Kohl, I.E. (2018). Assessing pyrite-derived sulfate in the mississippi river with four years of sulfur and triple-oxygen isotope data. Environ. Sci. Technol. *52*, 6126–6136. https://doi.org/10.1021/acs.est.7b05792.
124. Hemingway, J.D., Olson, H., Turchyn, A.V., Tipper, E.T., Bickle, M.J., and Johnston, D.T. (2020). Triple oxygen isotope insight into terrestrial pyrite oxidation. Proc. Natl. Acad. Sci. USA *117*, 7650–7657. https://doi.org/10.1073/pnas.1917518117.
125. Sun, T., Bao, H., Reich, M., and Hemming, S.R. (2018). More than ten million years of hyper-aridity recorded in the Atacama gravels. Geochim. Cosmochim. Acta *227*, 123–132. https://doi.org/10.1016/j.gca.2018.02.021.
126. Pettigrew, R.P., Priddy, C., Clarke, S.M., Warke, M.R., Stüeken, E.E., and Claire, M.W. (2021). Sedimentology and isotope geochemistry of transitional evaporitic environments within arid continental settings: from erg to saline lakes. Sedimentology *68*, 907–942. https://doi.org/10.1111/sed.12816.
127. Waldeck, A.R., Olson, H.C., Yao, W., Blättler, C.L., Paytan, A., Hodell, D.A., and Johnston, D.T. (2022). Calibrating the triple oxygen isotope composition of evaporite minerals as a proxy for marine sulfate. Earth Planet. Sci. Lett. *578*, 117320, https://doi.org/10.1016/j.epsl.2021.117320.
128. Fournier, G.P., Moore, K.R., Rangel, L.T., Payette, J.G., Momper, L., and Bosak, T. (2021). The archean origin of oxygenic photosynthesis and extant cyanobacterial lineages. Proc. Biol. Sci. *288*, 20210675, https://doi.org/10.1098/rspb.2021.0675.
129. Brocks, J.J., Logan, G.A., Buick, R., and Summons, R.E. (1999). Archean molecular fossils and the early rise of eukaryotes. Science *285*, 1033–1036. https://doi.org/10.1126/science.285.5430.1033.
130. Crowe, S.A., Døssing, L.N., Beukes, N.J., Bau, M., Kruger, S.J., Frei, R., and Canfield, D.E. (2013). Atmospheric oxygenation three billion years ago. Nature *501*, 535–538. https://doi.org/10.1038/nature12426.
131. Rasmussen, B., Fletcher, I.R., Brocks, J.J., and Kilburn, M.R. (2008). Reassessing the first appearance of eukaryotes and cyanobacteria. Nature *455*, 1101–1104. https://doi.org/10.1038/nature07381.
132. Shih, P.M. (2015). Photosynthesis and early earth. Curr. Biol. *25*, R855–R859. https://doi.org/10.1016/j.cub.2015.04.046.
133. Shih, P.M., Hemp, J., Ward, L.M., Matzke, N.J., and Fischer, W.W. (2017). Crown group Oxyphotobacteria postdate the rise of oxygen. Geobiology *15*, 19–29. https://doi.org/10.1111/gbi.12200.
134. Slotznick, S.P., Johnson, J.E., Rasmussen, B., Raub, T.D., Webb, S.M., Zi, J.W., Kirschvink, J.L., and Fischer, W.W. (2022). Reexamination of 2.5-ga "whiff" of oxygen interval points to anoxic ocean before goe. Sci. Adv. *8*, eabj7190, https://doi.org/10.1126/sciadv.abj7190.

135. Albut, G., Babechuk, M.G., Kleinhanns, I.C., Benger, M., Beukes, N.J., Steinhilber, B., Smith, A.J.B., Kruger, S.J., and Schoenberg, R. (2018). Modern rather than mesoarchaean oxidative weathering responsible for the heavy stable cr isotopic signatures of the 2.95 ga old ijzermijn iron formation (South Africa). Geochim. Cosmochim. Acta *228*, 157–189. https://doi.org/10.1016/j.gca.2018.02.034.

136. Rasmussen, B., Muhling, J.R., Suvorova, A., and Fischer, W.W. (2021). Apatite nanoparticles in 3.46–2.46 ga iron formations: evidence for phosphorus-rich hydrothermal plumes on early earth. Geology *49*, 647–651. https://doi.org/10.1130/G48374.1.

137. Ingalls, M., Grotzinger, J.P., Present, T., Rasmussen, B., and Fischer, W.W. (2022). Carbonate associated phosphate (cap) indicates elevated phosphate availability in Paleoproterozoic shallow marine environments. Geophys. Res. Lett. *49*, GL098100. https://doi.org/10.1029/2022GL098100.

138. Crockford, P., and Halevy, I. (2022). Questioning the paradigm of a phosphate-limited archean biosphere. Geophys. Res. Lett. *49*, e2022GL099818, https://doi.org/10.1029/2022GL099818.

139. Planavsky, N.J., Cole, D.B., Isson, T.T., Reinhard, C.T., Crockford, P.W., Sheldon, N.D., and Lyons, T.W. (2018). A case for low atmospheric oxygen levels during earth's middle history. Emerging Top. Life Sci. *2*, 149–159. https://doi.org/10.1042/ETLS20170161.

140. Bachan, A., and Kump, L.R. (2015). The rise of oxygen and siderite oxidation during the Lomagundi event. Proc. Natl. Acad. Sci. USA *112*, 6562–6567. https://doi.org/10.1073/pnas.1422319112.

141. Partin, C.A., Bekker, A., Planavsky, N.J., Scott, C.T., Gill, B.C., Li, C., Podkovyrov, V., Maslov, A., Konhauser, K.O., et al. (2013). Large-scale fluctuations in Paleoproterozoic atmospheric and oceanic oxygen levels from the record of u in shales. Earth Planet. Sci. Lett. *369*, 284–293. https://doi.org/10.1016/j.epsl.2013.03.031.

142. Hardisty, D.S., Lu, Z., Planavsky, N.J., Bekker, A., Philippot, P., Zhou, X., and Lyons, T.W. (2014). An iodine record of Paleoproterozoic surface ocean oxygenation. Geology *42*, 619–622. https://doi.org/10.1130/G35439.1.

143. Kipp, M.A., Stüeken, E.E., Bekker, A., and Buick, R. (2017). Selenium isotopes record extensivë marine suboxia during the great oxidation event. Proc. Natl. Acad. Sci. USA *114*, 875–880. https://doi.org/10.1073/pnas.1615867114.

144. Planavsky, N.J., Reinhard, C.T., Isson, T.T., Ozaki, K., and Crockford, P.W. (2020). Large massindependent oxygen isotope fractionations in mid-Proterozoic sediments: evidence for a lowoxygen atmosphere? Astrobiology *20*, 628–636. https://doi.org/10.1089/ast.2019.2060.

145. Prave, A.R., Kirsimäe, K., Lepland, A., Fallick, A.E., Kreitsmann, T., Deines, Yu.E., Romashkin, A.E., Rychanchik, D.V., Medvedev, P.V., Moussavou, M., et al. (2022). The grandest of them all: the Lomagundi–jatuli event and earth's oxygenation. J. Geol. Soc. *179*, jgs2021-036, https://doi.org/10.1144/jgs2021-036.

146. White, A.E., Giovannoni, S.J., Zhao, Y., Vergin, K., and Carlson, C.A. (2019). Elemental content and stoichiometry of sar11 chemoheterotrophic marine bacteria. Limnol. Oceanogr. Lett. *4*, 44–51. https://doi.org/10.1002/lol2.10103.

147. Hayes, J.M. (2004). An Introduction to Isotopic Calculations (Woods Hole Oceanographic Institution), p. 2543.

148. Des Marais, D.J., Strauss, H., Summons, R.E., and Hayes, J.M. (1992). Carbon isotope evidence for the stepwise oxidation of the Proterozoic environment. Nature *359*, 605–609. https://doi.org/10.1038/359605a0.

149. Pavlov, A.A., and Kasting, J.F. (2002). Mass-independent fractionation of sulfur isotopes in archean sediments: strong evidence for an anoxic archean atmosphere. Astrobiology *2*, 27–41. https://doi.org/10.1089/153110702753621321.

150. Zahnle, K., Claire, M., and Catling, D. (2006). The loss of mass-independent fractionation in sulfur due to a palaeoproterozoic collapse of atmospheric methane. Geobiology *4*, 271–283. https://doi.org/10.1111/j.1472-4669.2006.00085.x.

STAR★METHODS

KEY RESOURCES TABLE

REAGENT or RESOURCE	SOURCE	IDENTIFIER
Deposited data		
Crockford et al.; Data S1	This study	N/A
Software and algorithms		
Prism 9	Graphpad	N/A
Matlab 2019b	Mathworks, Crockford et al.[8]	N/A

RESOURCE AVAILABILITY

Lead contact

Further information and requests for resources should be directed to and will be fulfilled by the lead contact, Peter Crockford (petercrockford@cunet.carleton.ca).

Materials availability

This study did not generate new materials.

Data and code availability

- No new data was generated in this study. Compiled productivity estimates can be found in Data S2 or within the original studies cited in this manuscript.
- No new code was generated in this study.
- Any additional information required to reanalyze the data reported in this paper is available from the lead contact upon request.

All data utilized in this study can be found in the supplemental information. For additional information the lead contact will make this available through request.

EXPERIMENTAL MODEL AND SUBJECT DETAILS

No new data was generated in this study. Recalculation of productivity from $\Delta^{17}O$ results is described in method details section literature estimates and detailed methods can be found in refs Crockford et al.[8] and Cao and Bao.[116] Compiled productivity estimates and $\Delta^{17}O$ recalculation parameters can be found in Data S2.

METHOD DETAILS

Time bins

Literature estimates of primary productivity have been presented across a broad range of timescales. This range spans from individual stratigraphic layers to geologic eons. In the present study we divide the geologic record into 10 different time bins to group productivity estimates (bin time ranges are in Data S1). Within each bin we also consider whether major extinctions or global glaciations have been evidenced. For Phanerozoic extinctions we assign a conservative value of one million years for a productivity drop and subsequent recovery (Data S1). In the case of global glaciations, we rely on existing literature age estimates (Data S1). Within these intervals we set primary production to zero to provide a conservative estimate of historically integrated productivity. Time bins for our 'most probable' scenario is presented in Data S1, as are two different scenarios where the start of Bin 8 varies due to uncertainty regarding the rise of globally significant terrestrial land plants. We consider a scenario of early emergence of land plants at 450 Ma, coincident with the first land plant spores,[29] and a scenario of late rise of land plants at 350 Ma, coincident with evidence for the first forests.[28] We place the start of Bin 8 at 400 Ma for our 'most probable' scenario.

Bin 1 spans the origin of life to the emergence of globally significant anoxygenic photosynthesis at 3600 Ma. Across Bin 1 we follow estimates that are derived from the assumption that the global biosphere was fueled by chemoautotrophy and would have been electron donor limited. Bin 2 covers the rest of the Archean eon and into the earliest Proterozoic. Across Bin 2, most estimates typically assume that electron donor limitation regulated the size of the biosphere at this time[36,44,46,47,49] and these estimates are what characterizes this interval for our most-probable trajectory. However, we also consider work which has suggested that the global biosphere may have shifted into a nutrient-limited regime[37,41,51] potentially because of an early emergence of oxygenic photosynthesis prior to the GOE (Figure 1B).[21,22,24,117] We set the end of Bin 2 at 2450 Ma, which is consistent with several studies that

have suggested significant atmospheric oxygen accumulation in Earth's atmosphere at this time due to the disappearance of mass independently fractionated sulfur isotopes in the sedimentary record.[12,16,17] From Bin 3 onward oxygenic photosynthesis is assumed to dominate over all other types of autotrophy. Bin 3 spans Earth's Great Oxidation Event[52] between 2450 Ma to 2020 Ma. Bin 4 covers the latter half of the Paleoproterozoic and the Mesoproterozoic. Together these intervals are also colloquially termed the mid-Proterozoic. We define the end of the mid-Proterozoic (1050 Ma) to be consistent with the sulfate triple oxygen isotope record.[13] Bin 5 predominantly spans the Tonian period and terminates with the onset of the Sturtian glaciation.[31] Bin 6 spans the Cryogenian period. During this interval there are no literature productivity estimates that span the interglacial interval. We average Bin 5 and Bin 7 estimates and take the greatest uncertainty of either time interval as our upper and lower bounds for Bin 6 (Figure 1A). Bin 7 covers the earliest Ediacaran to the Paleozoic rise of land plants at 400 Ma in our 'most probable' scenario. Bin 8 spans the rise of globally significant land plants to the beginning of the Triassic period where algae whose chloroplasts were derived by secondary endosymbiosis from red algae have been inferred to begin to dominate marine productivity.[118] Bin 9 spans the Mesozoic. Bin 10 spans the Cenozoic to the present day.

Literature estimates

Our productivity compilation is presented in Data S2 and includes every explicit ancient productivity estimate put forward in the literature. In the case of previous estimates derived from triple oxygen isotope measurements ($\Delta^{17}O$) within sulfate minerals we recalculated productivity estimates with updated parameter values informed from recent advances in the understanding of this system which we describe in more detail below (Figure S1; Data S2). Studies were only omitted if they did not provide an original estimate (i.e., if they provided a previously published estimate), if there were significant internal inconsistencies in deriving a productivity estimate, or if inferences of productivity were not explicitly put forward and instead required multiple assumptions regarding ancient carbon cycling to derive this property. Specifically, with respect to the latter point (required assumptions), we did not translate productivity estimates from studies that have attempted to constrain organic carbon burial. Although changes to rates of organic carbon burial could be a response to changes in gross primary production, without additional constraints it is equally possible that such changes are responses to changes in organic matter respiration, remineralization or preservation in sediments. Under these considerations, 22 different studies were utilized for our synthesis. Our 'most probable' trajectory represents the geometric mean of estimates if their range was greater than a factor of 50 (Bins 1–5, 7) and a regular average otherwise (Bins 6, 8–10). Uncertainties on our compiled estimates span the absolute minimum to absolute maximum of lower and upper bounds on literature estimates (Data S2).

Recent advances in the understanding of $\Delta^{17}O$ signatures within sulfate warrants an updating of productivity measurements which can be generated from these data sets. Following the model of Cao and Bao,[116] the $\Delta^{17}O$ value of O_2 is the product of the concentrations of O_2 and CO_2 in the atmosphere and the biological flux of O_2 to the atmosphere which approximates gross primary productivity (cf. Liu et al. for an alternative interpretation).[119] The oxidation of sulfide in the environment can lead to product sulfate with a portion of its oxygen derived from atmospheric O_2, thus preserving a diluted atmospheric signature within the rock record. However, constraining the amount of oxygen that is incorporated into sulfate after initial sulfide oxidation, transport and preservation (f_{O2}) remains a challenge. Previous studies[8,13,42,119] have applied a calibration from pyrite oxidation experiments which suggest that 8%–15% of sulfate's oxygen is derived from O_2.[120] This calibration predicts that sulfate minerals will bear $\Delta^{17}O$ compositions between atmospheric O_2 and seawater sulfate (O_2, $-0.469‰$ relative to VSMOW[121]; SO_4, $-0.016‰$, relative to VSMOW.[122] However, measurements of modern sulfate depict a more complicated picture. For example, riverine measurements show conflicting results with Mississippi River waters having significant non-zero negative $\Delta^{17}O$ signatures (Figure S1),[123] but headwaters of the Himalaya having slightly positive $\Delta^{17}O$ signatures (Figure S1).[124] One possibility for observed ^{17}O enrichments is that some atmospheric SO_4 bearing a positive $\Delta^{17}O$ signature, is mixing in with Himalayan pyrite-derived sulfate. Indeed, sulfate minerals from the Atacama Desert which also have significant ^{17}O enrichments have followed this interpretation (Figure S1).[125] Beyond the Atacama, modern sulfates also preserve a wide range of $\Delta^{17}O$ values (Figure S1).[13] This range in values is possibly an expression of the natural variability inherent to the diversity of environments being sampled, but also the dissolution and redeposition of sulfate from ancient evaporite deposits.[126] Marine evaporites may offer a useful calibration point as they are a relatively consistent sedimentary facies in the rock record with respect to conditions amenable to their genesis. Recent study of Messinian sulfate provides a useful empirical calibration. Results from[127] shows that evaporites deposited during the Messinian salinity crisis only preserve a small portion of an atmospheric O_2 signature (1%; Figure S1). We take this result as an endmember and take the upper limit of experimental results[120] (15%) as our other endmember to constrain f_{O2}. In addition to changes in f_{O2} we also update atmospheric O_2 and CO_2 estimates across our different time bins. We input updated productivity results into our synthesis and present input parameters used calculate productivity values in Data S2.

In addition to our 'most probable' trajectory we also consider estimates that spawn from the possibility of a nutrient limited biosphere due to an early emergence of oxygenic photosynthesis. Evidence for Archean oxygenic photosynthesis has been argued for through molecular clocks,[128] biomarkers[129] and isotope geochemistry.[21,22,25,117,130] Under such a scenario, rates of primary production would have potentially increased compared to productivity estimates that have not included a contribution from this metabolism.[36,49] Indeed, models have been presented in which photosynthetic O_2 production up to tens of percent of modern productivity can be made consistent with atmospheric pO_2 10^{-5} present atmospheric levels, consistent with the presence of mass-independently fractionated sulfur isotopes in marine sedimentary rocks.[23,37] While oxygenic photosynthesis must have evolved before geochemical proxies record a rise of atmospheric O_2, whether oxygenic photosynthesis preceded atmospheric oxygenation by years or hundreds of millions of years remains highly debated. For example, the early evolution of oxygenic photosynthesis is questioned based on

molecular clocks, biomarkers and isotope geochemistry[131–135]—the same approaches used to propose such an early emergence. Moreover, recent work aimed at constraining nutrient levels in Archean oceans provide evidence that waters at this time were replete with phosphorus with concentrations above modern.[136,137] As model-based estimates of productivity have either assumed[37] or calculated phosphorus concentrations[41,50] in order to calculate productivity levels, these new geochemical observations[136,137] suggest such estimates may require revisiting and thus they are not included in our most probable trajectory.[138] Irrespective of this ongoing debate, we separate late Archean productivity estimates (Bin 2) into scenarios which assume a nutrient-limited biosphere with active oxygenic photosynthesis,[37,41,50] from one limited by electron donors (Data S2).[36,39,46,48,49] We plot these different trajectories in Figure 1 of the main text and extend estimates derived from a nutrient limited biosphere back to the earliest purported geochemical evidence for oxygenic photosynthesis at 3 Ga.[21,22,25,117,130]

Earth's Great Oxidation Event

In Figure 1 of the main text, we divide Bin 3 into both high-productivity and low-productivity scenarios. This division is motivated by the hypothesis of an atmospheric O_2 overshoot across Earth's Great Oxidation Event.[53] In an overshoot scenario, atmospheric O_2 levels rose to much higher levels than are inferred for the following mid-Proterozoic,[139] potentially exceeding modern levels.[140] Since this hypothesis was explicitly proposed,[53] numerous studies have argued for such an overshoot, utilizing various redox proxies applied to rocks deposited across this interval. To date, such evidence includes uranium enrichments in shales[141]; elevated iodine to calcium ratios in carbonate rocks[142]; selenium isotope enrichments[143]; and elevated carbon isotope ratios across part of this interval.[93] These high estimates of atmospheric O_2 concentrations, combined with sulfate triple oxygen isotope evidence, lead to extremely high levels of primary productivity during this interval of time.[13,116] Moreover, it has been argued that in any scenario of an O_2 overshoot, high primary productivity is a requisite criterion to create a stable Earth system state.[144]

In contrast to an O_2 overshoot, it is also possible that redox proxy evidence derived from the sedimentary record better reflects local conditions, temporally insignificant intervals of time, or diagenetic overprinting.[145] In such cases, a low-O_2 GOE scenario is equally permissible. In such a low-O_2 scenario, triple oxygen-based interpretations still require elevated primary productivity relative to the mid-Proterozoic interval.[8,13] However, productivity levels would be significantly reduced from the high-productivity GOE scenario. In the main text we consider as 'most probable' a low-productivity GOE scenario, leaning on both triple oxygen-based and model-based arguments for a low-O_2 Proterozoic world.[38,50]

Integrating productivity estimates

To derive the total productivity over Earth's history we multiplied the bin duration by the 'most probable' productivity value (geometric mean of estimates or average of estimates) and then summed results from all time bins. All estimates are presented relative to modern productivity. Therefore, to derive the total carbon fixed through primary production, we multiply our integrated productivity estimate by modern gross primary productivity 250 Gt C yr^{-1} (Figure S2A; see also Box 1). Results are presented and discussed in the main text for both high- and low-productivity GOE scenarios. We note that scenarios of high Archean productivity related to pre-GOE oxygenic photosynthesis, and high mid-Proterozoic productivity related to uncertainties in $\Delta^{17}O$-based reconstructions slightly increase estimates of total carbon fixed by the biosphere and the number of cells to have ever existed. Critically, the incorporation of such scenarios does not significantly impact any of the overall conclusions, which we present in the main text. Moreover, while we argue that these scenarios are less likely (see literature estimates above), we show their outcomes to account for the possibility that further study may find support for them.

Contributions to productivity through time

In the main text we evaluate chemoautotrophy + anoxygenic photosynthesis, cyanobacterial, algal and land plant contributions to global productivity through time. For chemoautotrophy + anoxygenic photosynthetic productivity contributions, we rely on Archean estimates of productivity, which only consider such metabolisms for our preferred trajectory. However, as we note above, we also consider an alternative scenario of an early emergence of oxygenic photosynthesis as far back as 3 Ga[21,22,25,117,130] and assume that the organisms utilizing this metabolism were cyanobacteria. For the interval of time after oxygenic photosynthesis emerged, we rely on Proterozoic, Phanerozoic, and modern estimates of the contributions of such metabolisms to global productivity.[56,46,145] For our 'most probable' trajectory we set the emergence of cyanobacterial productivity at the beginning of Bin 3, with the first sustained rise of atmospheric O_2, but also consider their emergence as early as 3 Ga for an alternative scenario.[21,22,25,117,130] For the rise of algae to ecological prominence we rely on reports of elevated sterane to hopane ratios in sedimentary rocks between 820 and 645 Ma.[18,20] Biomarker evidence is potentially consistent with zinc isotope data, which also place the rise of algae within the late Tonian.[19] For the rise of land plants, we place estimates consistent with charcoal records, fossil evidence for vascular plants and the earliest evidence for forests at 400 Ma.[29] As noted above, because it is difficult to translate fossil evidence to ecological prominence, we also consider an early rise of land plants coincident with land plant spores at 450 Ma and a late rise of land plants at the latest suggested emergence of forests at 350 Ma.[29] Upon terrestrial land plant colonization, we vary their contribution to global productivity between the range estimated over Pleistocene glacial-interglacial intervals.[6]

Constraining the proportion of algal versus cyanobacterial productivity is more challenging than assigning dates for emergence. In the modern ocean, cyanobacteria account for 25% of marine productivity[65] whereas algae contribute 75%. Of the algal contribution, red lineages, namely diatoms, coccolithphores and dinoflagellates, dominate. However, the makeup of marine algae has changed significantly since the late Tonian.[118] A limited deep marine sedimentary record—only extending back to the Mesozoic—makes

projecting the modern mosaic of marine productivity highly uncertain. While it is likely that green and not red algae dominated algal production in the late Proterozoic and Paleozoic, it is not clear what fraction of total production was algal. Given this uncertainty we consider multiple scenarios to evaluate what group likely dominated historical marine productivity. In our reference case we assume that it was not until modern forms of algae whose chloroplasts were derived by secondary endosymbiosis from red algae rose to dominate algal production that algae overtook cyanobacteria. In this scenario we assume an algal contribution of 25% of marine productivity until the Mesozoic. We also consider a scenario where algae rose to their modern level of marine dominance concurrent with biomarker records. Lastly, we consider a case where algal dominance only arose in the Cambrian. In concert with varying algal contributions to productivity we also vary land plant contributions to productivity, varying both timing of emergence and upper and lower estimates of their contribution. We present results and descriptions of different scenarios referenced above in Data S3 and provide figure panels visually representing these calculations (Figures S2A–S2C) and results in Figures S3A–S3F. It is important to note that we consider scenarios presented here to be conservative with respect to cyanobacterial contributions, as many factors may conspire to elevate their integrated relative contribution. These arguments are presented in the main text.

We find that no matter when significant algal or tree populations emerged, a high-productivity GOE trajectory leads to cyanobacterial dominance through time (Figures 1B and 1C main text; Figures S3A–S3F). Following a low-productivity GOE scenario, inferences become more nuanced. Irrespective of productivity over the GOE, scenarios of higher (cyanobacterial) Archean and/or mid-Proterozoic productivity than our most likely trajectory (Figure 1A) make it more likely that cyanobacteria dominated historical productivity. Across our low-productivity GOE path (Figure 1A), cyanobacteria achieve a plurality of historical productivity (i.e., a larger portion than land plants or algae but not a majority) only if algal productivity overtook cyanobacterial productivity in the earliest Mesozoic (250 Ma) and if modern levels of terrestrial productivity were achieved by the earliest Carboniferous (350 Ma). Although this is an end-member scenario, it is well supported with respect to algae if one assumes that algal dominance over cyanobacteria only took place when organisms such as diatoms became ecologically important. With respect to land plants, this scenario is supported if one assumes terrestrial productivity achieved modern levels concomitant with evidence for the rise of tree ferns (350 Ma).[29] In considering other possibilities, we only find that algae achieve a plurality of primary productivity if they reached modern-like marine productivity in the Proterozoic, coincident with elevated hopane/sterane ratios in the sedimentary record[18,20] and if land plants had a late emergence. However, we find that if land plants achieved modern levels of productivity before 400 Ma, then they would have achieved a plurality of historically integrated productivity across all other scenarios that assume a low-productivity GOE, including consideration of scenarios that assume an early and productive emergence of oxygenic photosynthesis as early as 3 Ga.[21,22,25,37,117,130]

Estimating the historically integrated cell population of the Earth

To derive an estimate for the total number of cells to have ever existed on Earth from our productivity estimates we begin with modern cell populations. Censuses of the modern biosphere depict the majority of Earth's standing stock cell population (i.e., every living cell on Earth today) as bacterial with $\approx 4\times10^{29}$ cells in marine sediments,[3,70] $\approx 2\times10^{29}$ cells in the oceanic crust,[71] $\approx 4\times10^{29}$ cells in the continental crust,[71] $\approx 3\times10^{29}$ cells in soils,[3,69] and $\approx 1\times10^{29}$ cells in marine waters,[3,69] meaning Earth's total cell population is $\sim10^{30}$ cells. However, due to the slow turnover times of the deep biosphere, and the relatively rapid turnover time of bacterial cells in the surface environment, marine autotrophs and heterotrophs dominate annual cell production with each producing $\sim10^{30}$ cell yr^{-1}.[65,69,72] That is, when considering new cells, or cell divisions over a year, populations with rapid turnover times can greatly surpass populations with very slow turnover times such as the subsurface, even if they possess a much larger standing stock cell population. Without knowing how ecosystem structure may have altered modern cell population distributions through deep time, we project modern annual cell production scaled to our productivity estimates.

To achieve our estimation, we convert productivity estimates through time to productivity years by normalizing to modern productivity. Next, we divide our approximation into two components, autotrophic cell numbers and heterotrophic cell numbers. For heterotrophs we assume that their population has scaled with productivity over Earth's past in the same way that it does today. Specifically, most heterotrophic cells in the modern ocean are small planktonic organisms, Sar-11 being the most abundant.[146] Here, we assume that small cells with large populations have existed alongside autotrophs since the origin of life and that their annual population is dependent upon annual primary production. For autotroph estimates, we assume that their global cell population has always been dominated by bacterial cells. We make this assumption based on two factors: cyanobacterial cells turn over on shorter timescales than algal cells, and due to their smaller size, more bacterial cells are required for the same output of productivity relative to algal cells. Together, these factors are why there are many more cyanobacterial cells in the ocean today than algal ones even though they contribute a smaller proportion of global marine productivity. Similarly, we neglect the terrestrial biosphere in this estimation. Again, although land plants are the largest contributor to global primary productivity today relative to algae or cyanobacteria, their large cell size and slow relative turnover makes their overall contribution to annual global cell production insignificant relative to the marine environment. Therefore, to estimate total autotroph cell numbers through time we account for both primary productivity through time but also the bacterial contribution to this productivity to derive our estimate. Finally, for both autotroph and heterotroph estimates, we multiply productivity years and combine both estimates to estimate a total cell population through time (Figure S2C). Results from calculations are presented in Data S4. We note that scenarios of high Archean productivity related to pre-GOE oxygenic photosynthesis, and high mid-Proterozoic productivity related to uncertainties in $\Delta^{17}O$-based reconstructions (Figure 1A), result in slightly higher cell population estimates. However, such estimates are not outside of the range covered by our uncertainty envelope (constructed from the range of individual productivity estimates), which we present in the main text.

Carbon cycling and carbon mass balance

Annually it is estimated that 0.1 Gt C is outgassed from the solid Earth.[43,98] To maintain long-term carbon mass balance, this outgassed carbon must either be deposited in the sedimentary reservoir on Earth's surface or be subducted to the mantle. Even slight imbalances between carbon outgassed and carbon buried, if left unchecked, would lead to inhospitable conditions on the surface Earth within relatively short timescales ($<10^6$ years). The two main sinks for carbon in the oceanatmosphere system are the burial of carbonate rock and organic matter. Elemental and isotopic mass balance in the ocean may be expressed as:[147]

$$dC/dt = V - B_{inorg} - B_{org},$$

$dC\delta/dt = V \times \delta_V - B_{inorg} \times \delta - B_{org} \times (\delta - \varepsilon)$, where C is the mass of carbon in the ocean-atmosphere, V is the volcanic outgassing source, and B_{inorg} and B_{org} are the carbonate and organic carbon burial sinks. V is the carbon isotopic composition of the volcanic source, δ is the isotopic composition of dissolved inorganic carbon (DIC) in the ocean, and ϵ is the fractionation of carbon isotopes associated with photosynthetic carbon fixation. At a steady state, the elemental mass balance reduces to $V = B_{inorg} + B_{org}$, and defining f_{org} as the fraction of organic matter burial out of the total carbon sink, the isotopic mass balance may be rearranged to give:

$$f_{org} = (\delta - \delta_V) / \epsilon.$$

In other words, given constraints on the carbon isotopic composition of the CO_2 outgassing source (δ_V) and on the carbon isotopic fractionation associated with photosynthesis (ϵ), measurements of the carbon isotopic composition of carbonate rocks (δ) may be used to estimate the fraction of organic matter burial out of the total carbon sink (f_{org}) at the rocks' time of deposition. Such an approach has been used to suggest that over Earth history 20-25% of carbon has been buried as organic matter and 75-80% as carbonate rock.[93,148] We note in the main text, that although this view of the carbon cycle can be reconciled with both carbon isotope records and our primary productivity synthesis for the post-GOE Earth, it cannot for the Archean. Specifically, the fluxes of organic matter burial inferred from the carbon isotopic record are greater than our productivity estimates by up to three orders of magnitude (Figure 2). Suggested variations in solid Earth degassing over time[94,95] do not substantially affect this imbalance (Figure 2).

There are multiple solutions to the problem presented above. First, productivity may have been much higher than we estimate here for the Archean Earth (Figure 1A).[99] One way of supporting much higher productivity is if oxygenic photosynthesis existed on the earliest Archean Earth, enabling levels of productivity significantly higher than previous estimates, which were based on the availability of electron donors.[36,44,46,47,49] Importantly, this scenario requires a balance of O_2 production and consumption, to prevent O_2 from rising to levels higher than the geochemical record suggests.[12,149,150] As an alternative to very early oxygenic photosynthesis, an Archean biosphere dominated by chemolithotrophy and anoxygenic photosynthesis may have been much more productive than previously estimated. Both in the case of oxygenic photosynthesis with more abundant and/or reactive O_2 sinks and in the case of a more productive non-oxygenic biosphere, fluxes of species such as H_2, H_2S and Fe^{2+}, would need to be orders of magnitude larger than previously estimated.[36,49] It is unclear whether such radical changes to the volcanic or hydrothermal supply of reduced species, but also of associated compounds (e.g., CO_2 in volcanic gases), is compatible with models of solid-Earth degassing or with a hospitable climate to life on the early Earth.

An alternative solution to the above apparent carbon mass imbalance is the recognition that the carbon isotopic composition of Archean carbonates may not be a faithful recorder of the global dissolved inorganic carbon pool, or that components of the Archean carbon cycle (e.g., the isotopic fractionation between CO_2 and organic matter) differed from today. In the first case, carbonate records are interpreted to better reflect local conditions or diagenetic overprinting and thus do not reflect the fractional burial of organic carbon. With numerous examples in the literature of both modern and ancient carbonates being significantly decoupled from open marine dissolved inorganic carbon,[101,103,145] we find this to be the most parsimonious solution to the apparent carbon imbalance (see the main text for further discussion).

QUANTIFICATION AND STATISTICAL ANALYSIS

Compiled estimates of productivity were weighted equally. Most probable estimates were taken as the geometric mean of estimates when the range between estimates exceeded a factor of 50 and as an average of estimates when the range between estimates was less than a factor of 50. Uncertainty envelopes for individual time bins are presented as either the minimum value presented for the lowest estimate or the maximum value presented for the highest estimate presented in the literature. Please refer to Data S2.